The Journal of Experimental Biology 208, 2913-2922
Published by The Company of Biologists 2005
doi:10.1242/jeb.01715

Mechanical properties of the integument of the common gartersnake, *Thamnophis sirtalis* (Serpentes: Colubridae)

Gabriel Rivera[1,*], Alan H. Savitzky[1] and Jeffrey A. Hinkley[2]

[1]*Department of Biological Sciences, Old Dominion University, Norfolk, VA 23529, USA* and [2]*Advanced Materials and Processing Branch, NASA Langley Research Center, Hampton, VA 23681, USA*

*Author for correspondence at present address: Department of Biological Sciences, Clemson University, Clemson, SC 29634, USA (e-mail: grivera@clemson.edu)

Accepted 28 May 2005

Summary

The evolution of the ophidian feeding mechanism has involved substantial morphological restructuring associated with the ability to ingest relatively large prey. Previous studies examining the morphological consequences of macrophagy have concentrated on modifications of the skull and cephalic musculature. Although it is evident that macrophagy requires highly compliant skin, the mechanical properties of the ophidian integument have received limited attention, particularly in the context of feeding. We examined mechanical properties of skin along the body axis in *Thamnophis sirtalis* (Colubridae). Data were collected from tensile tests and were analyzed using a multivariate analysis of variance (MANOVA) and *post-hoc* multiple comparison tests. Significant differences in mechanical properties were detected among regions of the body. In general, prepyloric skin is more compliant than postpyloric skin, consistent with the demands of macrophagy.

Key words: integument, skin, biomechanics, feeding, snake, *Thamnophis sirtalis.*

Introduction

The vertebrate integument serves a number of important roles, including functioning as a barrier to external pathogens, limiting desiccation and facilitating heat transfer with the environment (Frolich, 1997). In addition to these generalized static functions, the vertebrate integument serves a number of specialized dynamic functions typically associated with structural characteristics of the dermis (Parry and Craig, 1984; Craig et al., 1987; Frolich, 1997). The mechanical properties of skin are largely determined by the organization of dermal collagen and elastin fibers (Bischoff et al., 2000). Relatively stiff collagen fibers are the principal component determining the tensile strength of skin, whereas elastin fibers are primarily responsible for the recoiling of stretched skin (Hebrank, 1980; Hebrank and Hebrank, 1986; Oxlund et al., 1988). The mechanical properties of skin and their underlying structural characteristics have been examined in a broad array of vertebrate taxa, including sharks (Wainwright et al., 1978), bony fishes (Hebrank, 1980; Hebrank and Hebrank, 1986; Brainerd, 1994; Long et al., 1996), salamanders (Frolich et al., 1994), anurans (Greven et al., 1995; Zanger et al., 1995; Schwinger et al., 2001), bats (Swartz et al., 1996), gekkonid lizards (Bauer et al., 1989, 1992, 1993) and snakes (Jayne, 1988).

The evolution of snakes has involved considerable morphological change, including body elongation and the loss of limbs (Greene, 1997). Morphological adaptations of the skull and cephalic musculature, associated with the ability to ingest large-bodied prey, have been investigated extensively (Gans, 1961; Rieppel, 1980; Cundall, 1995; Lee et al., 1999; Cundall and Greene, 2000). In addition, recent studies have examined the mechanics of post-cranial prey transport (Moon, 2000; Kley and Brainerd, 2002). In order for slender-bodied organisms such as snakes to evolve a macrophagous feeding system, the esophagus, stomach, abdominal musculature and overlying integument must be modified to allow for considerable distension when accommodating large, intact prey (Gans, 1974; Arnold, 1983; Singh and Mittal, 1989; Mullin, 1996; Cundall and Greene, 2000). However, although it is evident that macrophagy in snakes requires highly compliant postcranial skin, the mechanical properties and morphological correlates of the ophidian integument have received limited attention, particularly in the context of feeding. Only one previous study (Jayne, 1988) has examined the mechanical properties of the ophidian integument. However, that study focused on the relevance of integumentary mechanics to locomotion. Jayne (1988) conducted tensile tests on skin samples by applying loads parallel to the longitudinal body axis for six species of snakes. Given the likely anisotropic behavior of ophidian skin, Jayne's results, although significant in the context of locomotion, provide few insights into the behavior of skin when stretched in the circumferential direction, as would occur during feeding.

The skin of snakes is unusual among vertebrate integuments in possessing folds of intersquamous skin between longitudinally oriented scale rows (Savitzky et al., 2004). The apparent function of these folds is to permit the maximum circumference of the snake to increase, allowing large-diameter prey to pass from the oral cavity into the stomach (Gans, 1952, 1974; Mullin, 1996). Snakes feeding on large prey typically possess a larger number of dorsal scale rows in prepyloric regions of the body than in postpyloric regions (Gans, 1974; Mullin, 1996; but see Shine, 2002). The greater number of scale rows and the associated folds of skin anterior to the pylorus allow undigested food to be accommodated more easily. Postpyloric regions require less circumferential stretch because food passing through the pylorus has been reduced in bulk.

Thamnophis sirtalis, the common gartersnake, belongs to the colubrid subfamily Natricinae and has an extensive distribution, extending between both coasts of North America (Rossman et al., 1996). Typically a habitat and prey generalist, its diet consists of both small- and large-diameter prey, including earthworms, fishes, amphibians, mammals and birds. Earthworms and amphibians typically constitute the largest proportion of the diet (Gregory, 1978; Rossman et al., 1996). In a Michigan population, earthworms were found to constitute 80% of the diet, while amphibians accounted for 15% (Carpenter, 1952).

Thamnophis sirtalis, like most snakes, has a resting body circumference that increases from the head toward the mid-body and then decreases toward the tail. Thus, within the prepyloric region of the trunk, which must accommodate undigested prey, the most anterior sections have the narrowest circumference. We hypothesize that, in response to the variation in body circumference and size of the food bolus, the skin should vary in its ability to stretch circumferentially in different regions along the length of the body. Such regional variation in the mechanical properties of skin that is subjected to different forces has been described in other taxa. Swartz et al. (1996) found that the skin of bat wings, which functions as the primary producer of lift and thrust during flight, varied in mechanical properties among the three regions of the wing membrane and suggested that this variation reflected the distinct role of each region during flight. In addition, we hypothesize that the biomechanical properties of the skin will change in association with the position of the pylorus, which separates prepyloric skin subjected to large food boluses from postpyloric skin that overlies the region of the digestive track in which prey has been reduced markedly in size. To test these hypotheses, we examined regional variation in the mechanical properties of the skin of *T. sirtalis* along the longitudinal body axis.

Materials and methods

Acquisition and processing of samples

Eleven common gartersnakes [*Thamnophis sirtalis* (L.)] were obtained from a commercial source (W. A. Lemberger Co., Inc., Oshkosh, WI, USA). Snakes were maintained at ambient laboratory temperature (18–24°C), fed a diet of earthworms and provided with water *ad libitum* until they were euthanized for mechanical testing. All snakes appeared in good health prior to testing. Eight male and three pre-reproductive female specimens of comparable size were used. Snout–vent length (SVL) ranged from 348 to 435 mm (mean, 385 mm) for males and 365 to 375 mm (mean, 368 mm) for females.

Each individual snake was weighed to the nearest 0.001 g using a top-loading electronic balance and was then euthanized by an intracardiac injection of sodium pentobarbital. SVL was measured to the nearest millimeter, and ventral scales were counted following the method described by Dowling (1951). A midventral incision was made along the length of the body. At both the anterior and posterior ends of the incision, a circumferential cut was made through the skin, completely detaching the body skin from that of the head and tail. To separate the skin from the body, the anterior edge was gently pulled caudally until the complete skin of the body was removed. The skin was spread on a flat surface, and transverse sections were cut using a razor blade. Nine circumferential strips of skin were prepared, each spanning 10 ventral scales. The excised strips were centered at increments of 10% of the ventral scale count (VSC); the initial strip of skin was excised at 10% and the final strip at 90% of the VSC. These regions were designated *a–i*, with *a* being the most anterior and *i* the most posterior (Fig. 1). Each excised strip was divided into equally wide anterior and posterior samples, and the edges of each sample were straightened using a razor blade to form smooth edges parallel to the direction of subsequent loading and extension and corresponding to the transverse body axis. For each individual snake, the anterior sample from each region was subjected to a uniaxial tensile test, and the posterior sample was preserved for histological preparation.

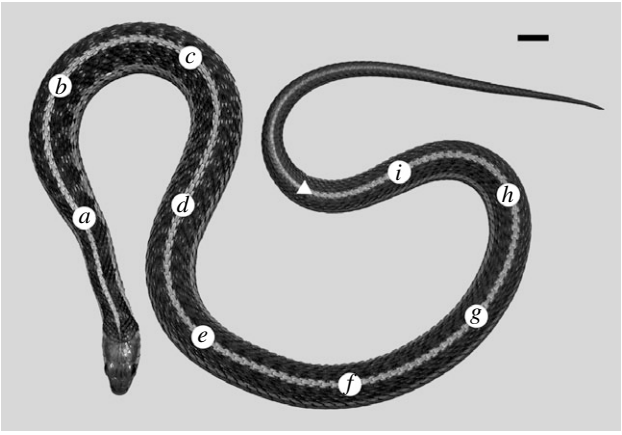

Fig. 1. Dorsal view of *Thamnophis sirtalis*. Circles mark the position at which each of the nine regions (*a–i*) is centered and are spaced at increments of 10% of the ventral scale count. The triangle indicates the level of the cloaca and represents 100% of the snout–vent length. Scale bar, 1 cm.

Determination of skin thickness

Skin thickness was measured from histological sections in order to quantify the cross-sectional area of samples subjected to mechanical tests. Samples were manually extended in the circumferential direction until taut. Samples were then pinned in this stretched condition to a vinyl sheet, fixed in 10% phosphate-buffered formalin and stored in 70% ethanol. For future morphometric analyses, including the quantification of dorsal scale rows, digital photographs of each fixed sample were taken.

For each individual snake, one subsample was removed from each of the nine regional samples. Each subsample was longitudinally centered within the sample and incorporated dorsal scale rows four through six of the right side. These scale rows were selected because they displayed relatively uniform scale dimensions and similar quantities of intersquamous skin (i.e. skin between the scales). Within each subsample, each of the three dorsal scale rows contained no fewer than two complete scales. Subsamples were prepared for histology using a Shandon Hypercenter XP automatic tissue processor (Pittsburgh, PA, USA). Subsamples were dehydrated through an ethanol series, cleared in xylene, embedded in a synthetic paraffin-polymer medium (Paraplast Plus; Oxford Labware/Sherwood Medical Co., St Louis, MO, USA) and serially sectioned at a thickness of 10 μm using a Leitz 1512 rotary microtome. Approximately 2 mm of tissue per subsample was sectioned from posterior to anterior. Sections were mounted on subbed slides, stained with iron gallein and counterstained with eosin (Presnell and Schreibman, 1997).

The stained sections were examined with a Nikon Optiphot compound microscope, and digital photographs were taken of the sections using an attached digital camera (Nikon Coolpix 990). After processing the digital images in Photoshop (version 6.0; Adobe Systems, Inc., San Jose, CA, USA), skin thickness was measured using SigmaScan Pro image analysis software (version 5.0; SPSS, Inc., Chicago, IL, USA), using the image of a stage micrometer for calibration. In order to obtain these measurements, serial sections were examined and the anterior progression of the posterior-most scale belonging to the fifth scale row was followed. This series revealed a transition from the unattached posterior tip of the scale to a point where the scale was completely attached to the intersquamous skin on both sides. At the latter point, the minimum thickness of the intersquamous skin was measured between scale row five and each of the two adjacent rows. Those two measurements were averaged to yield a single measure of thickness for the sample. By using the minimum skin thickness of each sample to calculate cross-sectional area, the results provide a conservative estimate of area but may overestimate the stress required to stretch skin circumferentially.

Dorsal scale rows

Regional variation in the number of dorsal scale rows was quantified from digital images of previously preserved skin samples using the method described by Peters (1964). The skin samples (N=108) were from 12 individual snakes: the 11 used for mechanical tests and one additional specimen.

Determination of in vivo *strain*

Three additional specimens were euthanized as previously described and regions *a–i* were located and marked on the intact specimen. Within the anterior half of each region (i.e. the half subjected to mechanical testing in the previous specimens), the *in situ* body circumference was measured to the nearest millimeter by wrapping cotton thread (Bellevue 16/4; American & Efird Thd. Mills, Inc., Mt Holly, NC, USA) around the body and marking both ends at a point where they overlapped. A linear measurement of the straightened string was made with digital calipers. The process was repeated three times for each region, yielding three independent measurements. These values were then averaged to yield a single value of *in situ* circumference for each region. Skin samples were excised from each region, as previously described, and placed on a smooth, moist glass surface. To prevent curling of the tissue, and to simulate the storage of samples used for mechanical analysis (see next section), a thin piece of glass was placed over the sample and a linear measurement of body circumference was recorded with digital calipers. This method facilitated the acquisition of accurate measurements and did not induce strain in the resting samples. The process was repeated three times for each region and those measurements were averaged to yield a single value of *ex situ* circumference. These data were used to determine the degree to which skin was strained *in vivo* and allowed for the normalization of any skewed strain data.

Mechanical testing

All samples used for mechanical analysis were positioned between folded strips of paper towel moistened with reptilian Ringer's solution (Guillette, 1982) and placed in a waterproof plastic container. The encased skin samples were saturated with Ringer's solution by filling the container, which was then placed on ice and transported to NASA Langley Research Center (Hampton, VA, USA) for mechanical testing. All samples were tested within 8 h of being excised (usually within 6 h). Skin samples were kept on ice until they were removed for measurement, at which time samples were submerged in a vial of reptilian Ringer's solution maintained at room temperature (22–24°C). Upon removal from the solution, the circumference, gage length (l_0) and width of each sample were measured to the nearest 0.01 mm using digital calipers (Mitutoyo America Corp., Aurora, IL, USA). Width was recorded as the maximum distance parallel to the longitudinal body axis. For measurements of circumference and gage length, moist skin samples were spread flat on a smooth glass surface and allowed to retract prior to recording data. Gage length was equal to the linear distance between the ventral edges of the first dorsal scale row of both the left and right sides (Fig. 2).

After linear measurements had been recorded, samples were resubmerged in reptilian Ringer's solution until they were tested. Each sample, measuring approximately 10×25 mm, was then mounted to screw-tightening aluminum grips and attached to the base and crosshead of the testing machine.

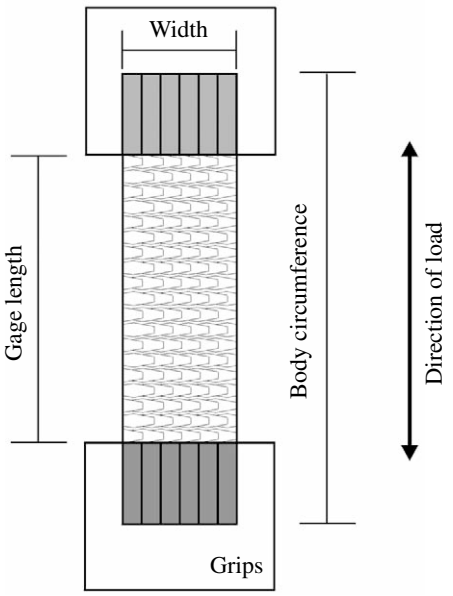

Fig. 2. Placement of the aluminum grips and direction of the applied load during mechanical tests. The load was applied along the long axis of the sample, which corresponds to the circumference of the body. Ventral scales are shaded.

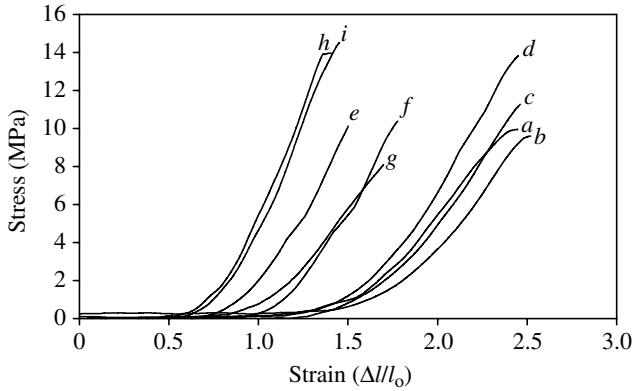

Fig. 3. Stress–strain curves for a single specimen (AHS L-9597). Curves were produced from data collected during uniaxial tensile tests. Each of the nine curves represents data collected from a single sample. Note the considerable strains attained (0.50–1.25) before appreciable stress is detected.

Uniaxial tensile tests were conducted using a vertical-loading Korros-Data materials testing machine (Sunnyvale, CA, USA), employing a 35 N load cell. Tests were conducted at room temperature (22–24°C). Prior to each test, the proximal edges of the two grips were preset to a distance of 5 mm. Uniaxial tensile tests were conducted to sample failure at an extension rate of 10 mm min^{-1}, with load applied parallel to the long axis of the rectangular samples (i.e. in the circumferential direction; Fig. 2). Load–extension data were collected at a rate of 1100 data points min^{-1} and were recorded on a personal computer using custom software developed in Power Basic (J.A.H.). Load was measured to the nearest 0.15 N, and extension, which was equal to crosshead displacement, was measured to the nearest 0.091 mm.

Data analysis

Recorded load–extension data were converted to text files (.txt) and imported into SigmaPlot (version 6.0; SPSS, Inc.). Data were smoothed using a polynomial regression, and weights calculated from the Gaussian density function with a sampling proportion of 0.05. Using a custom macro, initial loads were zeroed and subsequent values were adjusted accordingly. Stress (σ=N mm^{-2}=MN m^{-2}=MPa) was computed by dividing load values (N) by the cross-sectional area of the test sample (width × thickness in mm^2). Strains (ε) were calculated using extension data and the corresponding gage length. Because the distance preset between the grips (5 mm) was less than the gage length of each of the test samples, we scaled the strain data so that a strain of zero corresponded to the point when the inter-grip distance was equal to the linear measurement of gage length made prior to testing. Stress–strain curves were then generated from these data, with the results from each skin sample being translated into a single curve. Each individual snake had the potential to generate nine curves, representing the nine sample regions of the body (Fig. 3).

Mechanical data collected for each sample included the strains and instantaneous elastic moduli (E) at stresses of 1.0 and 2.0 MPa. Instantaneous elastic moduli were equal to the instantaneous slope of the curve at the points measured and were calculated using the 1st-derivative function macro of SigmaPlot (version 8.0). The macro computed the running average of 50 adjacent numerical derivatives.

All statistical analyses were performed using SPSS (version 10.0; SPSS, Inc.). In all two-way ANOVA and MANOVA analyses, regions were treated as fixed effects, and specimens (i.e. individuals) were treated as random effects. For data sets not meeting the assumptions of homogeneity of variances and normality, assumptions were satisfied by square-root transformation of the data. Variables showing significant regional effects were analyzed independently using a randomized-block ANOVA and Tukey multiple comparison test; the latter was used to identify homogeneous regional subsets. Unless stated otherwise, results are reported as means ± standard error of the mean (S.E.M.).

Results

Skin from 11 specimens was used for mechanical testing and in the determination of skin thickness. Of the 99 skin samples potentially available from these specimens for histology and mechanical testing, 98 were examined in the determination of skin thickness, and 93 were used in calculating mechanical results. Three additional specimens were used to assess *in vivo* strain.

Skin thickness

Thickness varied among individual samples from 0.019 to

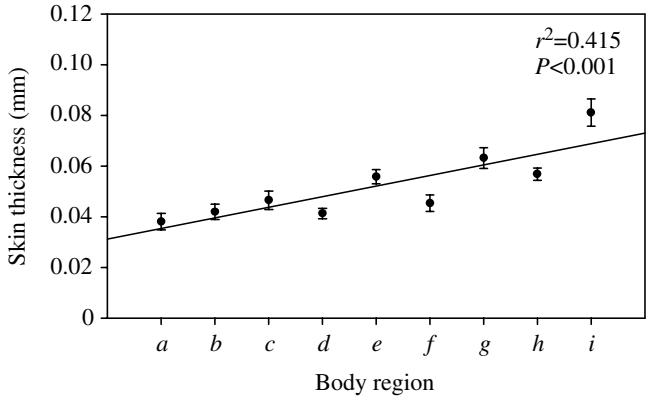

Fig. 4. Regional variation in skin thickness among body regions. Note the gradual increase in thickness posteriorly. Symbols represent means ± S.E.M. (N=11 for regions *a–h*; N=10 for region *i*).

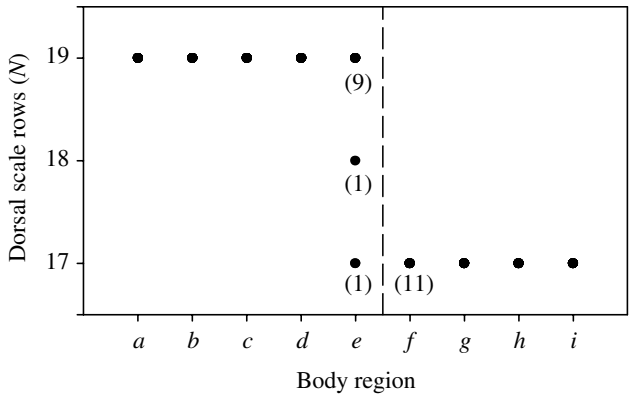

Fig. 5. Regional variation in number of dorsal scale rows. Scale-row reduction occurs at mid-body, approximately at the level of the pylorus. Data on scale rows were collected from 108 skin samples obtained from 12 specimens. Values in parentheses indicate the number of samples included for regions in which all 12 samples were not used. Two skin samples (one each for regions *e* and *f*) in transitional states of scale-row reduction were excluded from this data set. The location of the pylorus, between regions *e* and *f*, is indicated by a broken line.

0.107 mm. Skin was thinnest in anterior regions (0.038±0.003 mm for region *a*) and increased in thickness posteriorly (0.081±0.005 mm for region *i*; Fig. 4). Data were analyzed using a two-way randomized-block ANOVA, and significant differences among regions were found (F=20.111; d.f.=8,79; P<0.001). Results of a Tukey test indicated that, although there was nonclinal variation within the mid-body regions, the anterior-most (*a*), mid-body (*e*) and posterior-most (*i*) regions were significantly different from one another.

Dorsal scale rows

Scale-row reduction from 19 to 17 rows occurred in all specimens examined; 19 dorsal scale rows were present in regions *a–d*, and 17 were present in regions *f–i*. Region *e* represents a transitional region where 17, 18 and 19 scale rows were observed among the 12 specimens examined. Scale-row reduction involved the loss of scale row four on both the left and right sides and occurred between regions *d* and *f* (usually between regions *e* and *f*; Fig. 5).

In vivo *strain*

Twenty-seven skin samples from three specimens were analyzed using a repeated-measures ANOVA. No significant differences were detected between the *in situ* and *ex situ* measurements of circumference (F=0.103; d.f.=1; P=0.751). These results indicate that the skin is not significantly strained *in vivo*.

Mechanical tests

To detect significant differences among sample regions for all variables, mechanical data (strains and elastic moduli) were square-root transformed and analyzed using a two-way mixed-model MANOVA. Significant regional differences were detected (F=3.082; d.f.=32; P<0.001). Each variable was then analyzed independently using a randomized-block ANOVA. Significant regional differences were detected for all four variables (P<0.001; Table 1).

Mean strain values at both stresses (1.0 and 2.0 MPa) were highest in anterior regions (1.565±0.123 and 1.775±0.135 for region *a*, respectively) and decreased posteriorly (0.790±0.090 and 0.886±0.090 for region *i*, respectively; Fig. 6). These results indicate that the skin of anterior regions is more compliant than the skin of posterior regions. At both stresses, the anterior-most skin is capable of approximately twice the strain of the posterior-most skin. For both strain variables, mean values for each region were always less than the adjacent, more-anterior region. Results of separate regression analyses on both variables were significant. Mean strain at 2.0 MPa was slightly more strongly correlated with body region (r^2=0.534; P<0.001; Fig. 6) than strain at 1.0 MPa (r^2=0.487; P<0.001). For each strain variable, Tukey tests indicated that anterior regions *a–c* did not differ significantly from each other and that

Table 1. *Results of two-way mixed-model ANOVAs of mechanical data*

		Strain at 1.0 MPa		Strain at 2.0 MPa		Modulus at 1.0 MPa		Modulus at 2.0 MPa	
Effect	d.f.	F	P	F	P	F	P	F	P
Body region	8,74	**16.733**	**<0.001**	**19.510**	**<0.001**	**9.442**	**<0.001**	**11.191**	**<0.001**
Specimen	10,74	**6.302**	**<0.001**	**5.771**	**<0.001**	1.033	0.425	**2.892**	**0.004**

Significant results are shown in bold.

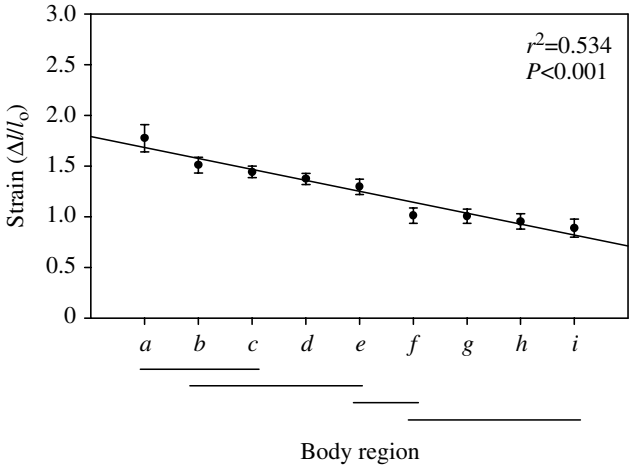

Fig. 6. Regional variation in strain at a stress of 2.0 MPa. Strain decreased posteriorly at a similar rate at both stress levels (1.0 and 2.0 MPa). Symbols represent means ± S.E.M. (*a*, *c*, *e*, *i*, *N*=10; *b*, *N*=9; *d*, *f*–*h*, *N*=11). Results of a Tukey multiple comparison test identify homogeneous regions.

posterior regions *f*–*i* did not differ significantly. However, the anterior regions (*a*–*c*) were significantly different from the posterior regions (*f*–*i*). In addition, although there was considerable overlap among the homogeneous subsets identified by the Tukey tests, the anterior-most (*a*), mid-body (*e*) and posterior-most (*i*) regions were all significantly different from each other at both levels of stress (Fig. 6).

Mean values for the elastic modulus at both stresses (1.0 and 2.0 MPa) were lower for anterior regions than for posterior regions, indicating that skin is more compliant in anterior regions and stiffer in posterior regions (Fig. 7). Mean modulus values at 1.0 MPa were lowest in region *a* (3.421±0.456 MPa) and highest in region *i* (9.0±0.552 MPa). Mean modulus values at 2.0 MPa were lowest for region *b* (6.180±0.507 MPa) and highest for region *g* (12.338±0.912 MPa; Fig. 7). Linear regression analyses were conducted on elastic moduli at both stresses and indicated a significant (P<0.001) relationship between body region and skin stiffness. Coefficients of determination were nearly equal for elastic moduli at 1.0 and 2.0 MPa (r^2=0.417 and 0.413, respectively). However, the coefficients were low in comparison to the strain data, in part because consecutive regions did not consistently increase posteriorly. Results from Tukey tests at both stresses indicate that mean moduli for regions *a*–*e* comprise a homogeneous subset that differs significantly from a second homogeneous subset consisting of regions *f*–*i* (Fig. 7). To determine the relationship of these two homogeneous groups to the location of the pylorus, which marks the posterior end of the stomach, two specimens were dissected and the pylorus was located. The pylorus lies between regions *e* and *f*, and therefore between the two regional groups defined by integumentary mechanics.

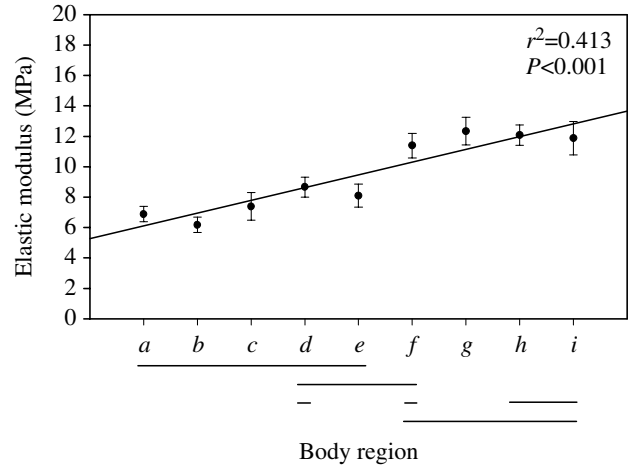

Fig. 7. Regional variation in elastic modulus at a stress of 2.0 MPa. Elastic moduli increased posteriorly at a similar rate at both stress levels. A distinct increase exists between the moduli of anterior regions (*a*–*e*) and posterior regions (*f*–*i*) at both stresses, indicating a sharp increase in skin stiffness. Symbols represent means ± S.E.M. (*a*, *c*, *e*, *i*, *N*=10; *b*, *N*=9; *d*, *f*–*h*, *N*=11). Results of a Tukey multiple comparison test identify homogeneous regions.

The circumference (c) of each skin sample at 2.0 MPa was calculated using the formula:

$$c_{\text{stretched}} = c_{\text{rest}} + \varepsilon_{\sigma} \times l_{\text{o}} ,$$

where ε_{σ} is the strain at a given stress, and l_{o} is the gage length (i.e. original length). Calculated values ($c_{\text{stretched}}$) were compared with the circumference of the same samples at rest (c_{rest}). Within the prepyloric trunk (regions *a*–*e*), mean circumference is considerably larger and relatively less variable at 2.0 MPa (mean ± S.D., 41.05±3.04 mm) than at rest (mean ± S.D., 23.64±2.24 mm; Fig. 8). The circumferential data at 2.0 MPa were analyzed using a randomized-block ANOVA, and significant differences were found among regions (F=107.628; d.f.=8,74; P<0.001). Results of a Tukey test indicate that, although regions *a*–*e* do not comprise an entirely homogeneous group, the anterior and posterior ends of

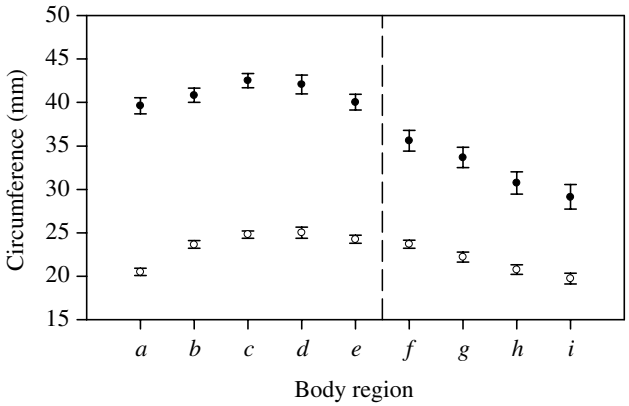

Fig. 8. Regional variation in body circumference at rest and at a constant stress of 2.0 MPa. Open circles represent circumference at rest; solid circles represent circumference at constant stress. Symbols represent means ± S.E.M. The location of the pylorus relative to the nine regions of the body is indicated (broken line) and was determined by dissection of two specimens.

the prepyloric trunk (regions *a* and *e*, respectively) do not differ significantly. Additionally, each of the five prepyloric regions is significantly different from regions *f–i*.

Discussion

Comparison with previous integumentary studies

The skin of *Thamnophis sirtalis* tested in the circumferential direction is considerably more extensible than the skin tested longitudinally by Jayne (1988). For the 49 samples tested by Jayne, strain at the end of failure ranged between 0.17 and 0.69. These values are considerably lower than the strains recorded in this study at the relatively low stresses of 1.0 and 2.0 MPa. The latter represents 35.5% of the mean stress at failure for region *a* and 15.4% for region *i*. Strains at 2.0 MPa for individual samples ranged from 1.05 to 2.475 (mean, 1.775) for region *a*, and 0.544–1.372 (mean, 0.886) for region *i*. In addition, 88 of the 93 samples for which data were analyzed did not elicit appreciable stress until strains had exceeded 0.5; the five samples that did were from posterior regions (*f–i*). Of the vertebrates for which mechanical properties of the integument have been studied, only the skin of the pufferfish, *Diodon holocanthus*, shows comparable extensibility. Brainerd (1994) found that the skin of *D. holocanthus* could attain strains of 0.4 without detectable forces being exerted.

Whereas Jayne (1988) found only slight differences in skin mechanics among dorsoventral locations within a specimen when subjected to longitudinal loading, this study found that differences among anteroposterior regions were highly significant in response to circumferential loading. Although the contrasting results may reflect differences in skin morphology among the species examined (*Thamnophis sirtalis* in this study *vs* six species in Jayne, 1988), we suspect that the direction in which the load was applied (i.e. circumferential *vs* longitudinal) had a much larger effect. Skin of another elongate vertebrate, the American eel (*Anguilla rostrata*), has been shown to be anisotropic (Hebrank, 1980). The mean terminal elastic modulus for the skin of eels tested in the circumferential direction was an order of magnitude larger (1.47×10^7 N m^{-2}) than the modulus for skin tested in the longitudinal direction (3.54×10^6 N m^{-2}). The existing data indicate that snakes differ from eels in the direction in which the skin is stiffer.

Thamnophis sirtalis has considerably more extensible skin than do geckos, the only other squamate group for which mechanical data on skin are available. Bauer et al. (1989) found that the skin of two species of geckos, *Ailuronyx seychellensis* and *Gecko gecko*, had mean failure strains (ε_f) of 0.31 and 0.57, respectively, tested in the longitudinal direction.

Mechanics of snake skin

The skin of *Thamnophis sirtalis* exhibits substantial variation in its mechanical properties among regions of the body. Mean strain was highest in the anterior-most region of the body and decreased caudally. At both stresses (1.0 and 2.0 MPa), strains for region *i* were approximately 50% (0.505 and 0.499, respectively) of the strains attained for region *a*. Tukey tests demonstrated that regional differences in strain were sufficient to identify significantly different anterior (*a*), mid-body (*e*) and posterior (*i*) regions, despite considerable overlap among immediately adjacent regions.

The elastic modulus (i.e. stiffness) of the skin increased two- to three-fold between regions *a* and *i*. A substantial increase in skin stiffness is observed posterior to the pylorus (i.e. behind region *e*). Tukey tests for the elastic moduli at both stress levels found significant differences between the prepyloric regions (*a–e*) and the postpyloric regions (*f–i*). This difference in mechanical properties is not surprising. Like most snakes, *Thamnophis sirtalis* consumes its prey intact, and the bolus is reduced in the stomach prior to passage through the pylorus into the intestine. Therefore, the posterior skin need not be capable of extension as great as that of the anterior skin. Because *T. sirtalis* is viviparous, it is possible that reproductive females experience different selective pressures in regard to the ability of the posterior skin to stretch, associated with an increase in embryonic size during gestation. While beyond the scope of this paper, subsequent studies could seek to determine whether mechanical differences exist between the skin of reproductively mature male and female snakes.

This study attempted to examine mechanical properties of the ophidian integument in a biologically relevant context. Tensile tests were conducted at temperatures within the range at which *Thamnophis sirtalis* is active and known to feed in nature (Carpenter, 1956; Nelson and Gregory, 2000). The use of rectangular strips of tissue produced a more uniform stress on the sample during loading and allowed crosshead displacement to be related directly to sample strain, particularly at the low stresses reported here (Edsberg et al., 1999; Foutz et al., 1992). Furthermore, because properties of the skin may vary from the ventrolateral to the middorsal regions, the use of complete circumferential strips is more likely to reflect behavior of the skin *in vivo*. Uniaxial tensile tests were conducted to the point of skin failure. However, due to the nontapered shape of the mechanically tested skin samples, severe necking occurred at high stresses and failure of samples occurred at or near the grips in 61 of the 93 (65.6%) tensile tests. Shearing of the grip-fastened skin occasionally occurred at high stresses; however, by visually monitoring the extension of each skin sample, it was determined that the mechanical data were not affected by shearing or slippage at the low stresses reported. Nonetheless, because of these complications, failure strains and maximum stresses were not considered accurate or biologically informative. The measurement of skin thickness from histological sections was necessitated by the complex, heterogeneous structure of ophidian skin. While the use of ethanol in the preparation of the histological samples may have induced shrinkage, any effects should be constant across all skin samples, and thus do not impact our conclusions. In addition, the use of formalin-fixed histological sections for determining skin thickness has been employed in other studies of vertebrate integumentary mechanics (Bauer et al., 1992; Bauer et al., 1993) and provides more accurate values of stress

than the method of measuring minimum skin thickness employed by Jayne (1988).

It is probable that data collected using biaxial tensile tests would more accurately reflect *in vivo* strain and stiffness values. However, the intention of this paper is not to describe the exact quantitative properties of skin *in vivo* but rather to describe the relative pattern of skin extensibility among longitudinal regions of the body. We believe that the quantitative differences observed among regions within our data provide valid comparisons. In addition, because the majority of studies examining the mechanical properties of vertebrate integument have used only uniaxial tensile tests (Jayne, 1988; Bauer et al., 1989, 1992, 1993; Brainerd, 1994; Greven et al., 1995; Zanger et al., 1995; Swartz et al., 1996; Schwinger et al., 2001), our use of this method allows for comparisons across taxa.

Our comparison of *in situ* and *ex situ* circumference supports the use of linear measurements of circumference. Biological materials are often pre-strained *in vivo*, and when samples of such tissues are excised, contraction may result in the inflation of observed strains. However, we observed no significant differences between the two series of skin measurements. We therefore conclude that the skin of *Thamnophis sirtalis* is not substantially strained *in vivo* and that the lengths of the excised samples accurately reflected the resting circumference of each region. For an organism that requires substantial extension of the skin when it feeds, it seems reasonable that no appreciable *a priori* strain exists, since such a resting strain would reduce the possible circumferential distention when prey is consumed.

Integumentary morphology

Along the length of the body, the mean skin thickness of *Thamnophis sirtalis* varies by a factor of more than two. Skin is thinnest in the anterior-most region of the body (region *a*) and increases caudally, concomitant with the gradient in decreasing compliance. Although the overall data show a negative relationship between strain and skin thickness (Fig. 9), weak positive relationships exist within seven of the nine regions (*a–e*, r^2=0.00–0.09; *f*, r^2=0.41; *g*, r^2=0.19). This suggests that regional differences in the integument other than variation in thickness along the body axis may influence the mechanical function of the skin. Such differences may include the number of dorsal scale rows, the quantity of intersquamous skin, and the angle formed between adjacent scale rows (Savitzky et al., 2004). In some macrostomate taxa, it has been argued that higher numbers of dorsal scale rows are associated with a greater capacity for stretching (Gans, 1974; Pough and Groves, 1983; Mullin, 1996). Shine (2002) found that high numbers of mid-body scale rows were significantly related to the proportion of the diet consisting of mammals. However, when body size of the snake was accounted for, the results were not significant. We suggest that a better integumentary predictor of prey diameter is the pattern of scale-row reduction. Rather than simply examining the number of dorsal scale rows at mid-body, a more appropriate approach may be to examine the number of mid-body scale rows relative to the number of anterior rows. *Thamnophis sirtalis* has 19 dorsal scale rows in regions *a–d* and 17 rows in regions *f–i*. The location of this scale-row reduction corresponds fairly closely to the location of the pylorus, where skin stiffness noticeably increases. The relative change in strain and elastic modulus that corresponds to the transition between regions *e* and *f* represents the single largest change between two sequential regions (Table 2). For values of the modulus, the magnitude of this change was more than twice that seen between any other adjacent regions.

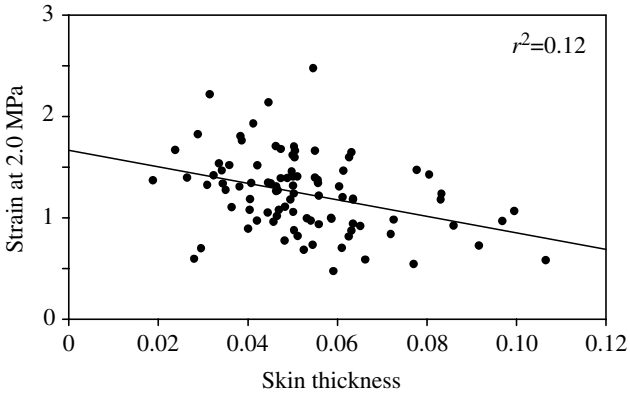

Fig. 9. Relationship between skin thickness and the strain attained at a constant stress (2.0 MPa) for each of the 93 samples for which mechanical data were collected.

Here, we propose a possible mechanism for the marked decrease in compliance observed between regions *e* and *f*. We suggest that scale row reduction impacts skin extensibility by decreasing the potential amount of intersquamous skin that is available to be stretched. The skin, which is present as folds in anterior regions, permits greater circumferential extension of the skin as the folds are straightened. It is possible, therefore, that initial strains are not the result of stressing a taut material but rather are associated with unfolding. This would help

Table 2. *Differences in mechanical properties between adjacent regions*

Region interface	Strain at 2.0 MPa		Modulus at 2.0 Mpa	
	Change	% Change	Change	% Change
a/*b*	(–) 0.265	14.93	(–) 0.706	10.25
b/*c*	(–) 0.069	4.57	(+) 1.212	19.61
c/*d*	(–) 0.068	4.72	(+) 1.270	17.18
d/*e*	(–) 0.079	5.75	(–) 0.562	6.49
e/*f*	(–) 0.283	21.87	(+) 3.292	40.64
f/*g*	(–) 0.006	0.59	(+) 0.946	8.30
g/*h*	(–) 0.053	5.27	(–) 0.254	2.06
h/*i*	(–) 0.066	6.93	(–) 0.211	1.75

Change represents the difference between means of each region.

Sign values (+/–) describe the direction of change in values from anterior to posterior.

The largest change between adjacent regions occurs between regions *e* and *f*, coinciding with scale-row reduction.

explain why the initial extension of the skin occurs with relatively little resistance (Fig. 3). This mechanism for allowing large extensions is different from that described by Brainerd (1994) for comparable skin extension in the puffer fish, *Diodon holocanthus*, for which no macrofolds of skin were observed but rather where folded collagen fibers are the structural innovation. Additionally, regional differences in dermal ultrastructure, such as diameters and orientation of collagen fibers within the intersquamous skin, may have a substantial impact on the ability of skin to stretch once unfolded. While beyond the scope of this paper, future studies are planned to examine regional variation in the structure of the ophidian dermis.

The role of skin in feeding

If the maximum circumference attainable during feeding resulted only from the extensibility of the skin, then large food items would meet gradually increasing integumentary resistance as they moved through the esophagus and stomach toward the pylorus. However, the maximum circumference attainable to accommodate prey is the result of two factors, skin extensibility and body circumference at rest. As skin extensibility decreases within regions *a–e*, resting body circumference correspondingly increases. This increase in resting body circumference within regions *a–e* partially compensates for the concomitant decrease in skin compliance, resulting in a higher, less variable maximum attainable circumference during feeding; such a result was predicted by Cundall and Greene (2000). Posterior to region *e,* body circumference decreases caudally as skin compliance continues to decrease. The combination of these two factors results in a rapid decrease in the attainable circumference within postpyloric regions, where food items have already been reduced in mass.

Phylogenetic trends

Although the skin of *Thamnophis sirtalis* shows a remarkable capacity for stretching, it is likely that the skins of certain other species of snakes have an even greater capacity. Viperid snakes show numerous morphological adaptations for feeding on very large prey, including modifications in cranial structure and body shape (Pough and Groves, 1983). Although gape obviously represents the first limiting factor in consuming large prey (King, 2002), the extensibility of the skin and certain internal structures, such as the gut, are also potential constraints. However, it is counterintuitive that the external skin would evolve the capacity to accommodate large-diameter prey without concomitant adaptations of internal structures. With respect to macrophagy, a parallel examination of cranial and integumentary morphology in basal and advanced alethinophidian snakes should be conducted to determine whether a correlation exists between gape size and characters associated with circumferential distention. Likewise, a phylogenetic analysis of the biomechanical properties of skin may reveal patterns related to the transition to macrostomy.

If the regional trends in integumentary structure observed in *Thamnophis sirtalis* are typical of macrostomate snakes, an examination of the integument of basal alethinophidian snakes, which are obligate consumers of slender prey (Greene, 1997), may reveal a different pattern. For snakes that do not require highly extensible skin, regional variation may be minimal. Furthermore, many basal taxa have a relatively cylindrical body shape. These factors suggest that the skin of these snakes may be more homogeneous along the length of the body.

This study is the first to provide quantitative evidence demonstrating that skin compliance varies regionally within snakes. We also provide the first mechanical evidence that variation in the properties of skin varies with the demands of macrophagy. Thickness of the skin co-varies with compliance and may be one of its major determinants. Within prepyloric regions, compliance shows an inverse relationship with resting body circumference. Additionally, postpyloric skin is significantly stiffer than prepyloric skin. Scale row reduction, which occurs near the level of the pylorus, coincides with a substantial increase in skin stiffness, perhaps resulting from a reduction in the amount of intersquamous skin due to the loss of one scale row from each side of the body. Further histological and mechanical investigations may shed additional light on the evolution of the ophidian dermis and the diversity that exists among both basal and macrostomate snakes.

Victor R. Townsend, Jr provided invaluable help and advice, particularly with skin sampling and histological protocols. We thank Angela Rivera, Monica McGarrity and Deborah Hutchinson for their help, support and advice over the past three years. Mark Butler and William Resetarits provided statistical advice and allowed the use of essential equipment. Adam Summers provided early comments that greatly improved this study, and Richard Blob and two anonymous reviewers helped us improve upon an earlier draft of this paper. Mechanical testing was conducted at NASA Langley Research Center. This work was supported in part by NSF DBI-9876817 to A.H.S. and William A. Velhagen, Jr and by a Sigma Xi Grant-in-Aid-of-Research to G.R.

References

Arnold, S. J. (1983). Morphology, performance and fitness. *Am. Zool.* **23**, 347-361.

Bauer, A. M., Russell, A. P. and Shadwick, R. E. (1989). Mechanical properties and morphological correlates of fragile skin in gekkonid lizards. *J. Exp. Biol.* **145**, 79-102.

Bauer, A. M., Russell, A. P. and Shadwick, R. E. (1992). Skin mechanics and morphology in *Sphaerodactylus roosevelti* (Reptilia: Gekkonidae). *Herpetologica* **48**, 124-133.

Bauer, A. M., Russell, A. P. and Shadwick, R. E. (1993). Skin mechanics and morphology of two species of *Pachydactylus* (Reptilia: Gekkonidae). *S.-Afr. Tydskr. Dierk.* **28**, 192-197.

Bischoff, J. E., Arruda, E. M. and Grosh, K. (2000). Finite element modeling of human skin using an isotropic, nonlinear elastic constitutive model. *J. Biomech.* **33**, 645-652.

Brainerd, E. L. (1994). Pufferfish inflation: functional morphology of postcranial structures in *Diodon holocanthus* (Tetraodontiformes). *J. Morphol.* **220**, 243-261.

Carpenter, C. C. (1952). Comparative ecology of the common garter snake (*Thamnophis s. sirtalis*), the ribbon snake (*Thamnophis s. sauritus*), and

Butler's garter snake (*Thamnophis butleri*) in mixed populations. *Ecol. Monogr.* **22**, 235-258.

Carpenter, C. C. (1956). Body temperatures of three species of *Thamnophis*. *Ecology* **37**, 732-735.

Craig, A. S., Eikenberry, E. F. and Parry, D. A. D. (1987). Ultrastructural organization of skin: classification on the basis of mechanical role. *Connect. Tissue Res.* **16**, 213-223.

Cundall, D. (1995). Feeding behaviour in *Cylindrophis* and its bearing on the evolution of alethinophidian snakes. *J. Zool. Lond.* **237**, 353-376.

Cundall, D. and Greene, H. W. (2000). Feeding in snakes. In *Feeding: Form, Function, and Evolution in Tetrapod Vertebrates* (ed. K. Schwenk), pp. 293-333. San Diego: Academic Press.

Dowling, H. G. (1951). A proposed standard system of counting ventrals in snakes. *Br. J. Herpetol.* **1**, 97-99.

Edsberg, L. E., Mates, R. E., Baier, R. E. and Lauren, M. (1999). Mechanical characteristics of human skin subjected to static versus cyclic normal pressures. *J. Rehabil. Res. Dev.* **36**, 133-141.

Foutz, T. L., Stone, E. A. and Abrams, C. F., Jr (1992). Effects of freezing on mechanical properties of rat skin. *Am. J. Vet. Res.* **53**, 788-792.

Frolich, L. M. (1997). The role of the skin in the origin of amniotes: permeability barrier, protective covering and mechanical support. In *Amniote Origins: Completing the Transition to Land* (ed. S. S. Sumida and K. L. M. Martin), pp. 327-352. San Diego: Academic Press.

Frolich, L. M., LaBarbera, M. and Stevens, W. P. (1994). Poisson's ratio of a crossed fibre sheath: the skin of aquatic salamanders. *J. Zool. Lond.* **232**, 231-252.

Gans, C. (1952). The functional morphology of the egg-eating adaptations in the snake genus *Dasypeltis*. *Zoologica* **37**, 209-248.

Gans, C. (1961). The feeding mechanism of snakes and its possible evolution. *Am. Zool.* **1**, 217-227.

Gans, C. (1974). *Biomechanics, an Approach to Vertebrate Biology.* Philadelphia: Lippincott.

Greene, H. W. (1997). *Snakes: the Evolution of Mystery in Nature.* Berkeley: University of California Press.

Gregory, P. T. (1978). Feeding habits and diet overlap of three species of garter snakes (*Thamnophis*) on Vancouver Island. *Can. J. Zool.* **56**, 1967-1974.

Greven, H., Zanger, K. and Schwinger, G. (1995). Mechanical properties of the skin of *Xenopus laevis* (Anura, Amphibia). *J. Morphol.* **224**, 15-22.

Guillette, L. J., Jr (1982). A physiological (Ringer's) solution for anoline lizards. *Herpetol. Rev.* **13**, 37-38.

Hebrank, M. R. (1980). Mechanical properties and locomotor functions of eel skin. *Biol. Bull.* **158**, 58-68.

Hebrank, M. R. and Hebrank, J. H. (1986). The mechanics of fish skin: lack of an "external tendon" role in two teleosts. *Biol. Bull.* **171**, 236-247.

Jayne, B. C. (1988). Mechanical behaviour of snake skin. *J. Zool. Lond.* **214**, 125-140.

King, R. B. (2002). Predicted and observed maximum prey size-snake size allometry. *Funct. Ecol.* **16**, 766-772.

Kley, N. J. and Brainerd, E. L. (2002). Post-cranial prey transport mechanisms in the black pinesnake, *Pituophis melanoleucus lodingi*: an x-ray videographic study. *Zoology* **105**, 153-164.

Lee, M. S. Y., Bell, G. L., Jr and Caldwell, M. W. (1999). The origin of snake feeding. *Nature* **400**, 655-659.

Long, J. H., Jr, Hale, M. E., McHenry, M. J. and Westneat, M. W. (1996). Functions of fish skin: flexural stiffness and steady swimming of longnose gar *Lepisosteus osseus*. *J. Exp. Biol.* **199**, 2139-2151.

Moon, B. (2000). The mechanics of swallowing and the muscular control of diverse behaviours in gopher snakes. *J. Exp. Biol.* **203**, 2589-2601.

Mullin, S. J. (1996). Adaptations facilitating facultative oophagy in the gray rat snake, *Elaphe obsolete spiloides*. *Amphibia-Reptilia* **17**, 387-394.

Nelson, K. J. and Gregory, P. T. (2000). Activity patterns of garter snakes, *Thamnophis sirtalis*, in relation to weather conditions at a fish hatchery on Vancouver Island, British Columbia. *J. Herpetol.* **34**, 32-40.

Oxlund, H., Manschot, J. and Viidik, A. (1988). The role of elastin in the mechanical properties of skin. *J. Biomech.* **21**, 213-218.

Parry, D. A. D. and Craig, A. S. (1984). Growth and development of collagen fibrils in connective tissue. In *Ultrastructure of the Connective Tissue Matrix* (ed. A. Ruggeri and P. M. Motta), pp. 34-64. Boston: Martinus Nijhoff.

Peters, J. A. (1964). *Dictionary of Herpetology.* New York: Hafner Publishing.

Pough, F. H. and Groves, J. D. (1983). Specializations of the body form and food habits of snakes. *Am. Zool.* **23**, 443-454.

Presnell, J. K. and Schreibman, M. P. (1997). *Humason's Animal Tissue Techniques,* fifth edition. Baltimore: Johns Hopkins University Press.

Rieppel, O. (1980). The evolution of the ophidian feeding system. *Zool. Jahrb. Abt. Anat. Ontog. Tiere* **103**, 551-564.

Rossman, D. A., Ford, N. B. and Seigel, R. A. (1996). *The Garter Snakes: Evolution and Ecology.* Norman: University of Oklahoma Press.

Savitzky, A. H., Townsend, V. R., Jr, Hutchinson, D. A. and Mori, A. (2004). Dermal characteristics, scale row organization, and the origin of macrostomy in snakes. *J. Morphol.* **260**, 325.

Schwinger, G., Zanger, K. and Greven, H. (2001). Structural and mechanical aspects of the skin of *Bufo marinus* (Anura, Amphibia). *Tissue Cell* **33**, 541-547.

Shine, R. (2002). Do dietary habits predict scale counts in snakes? *J. Herpetol.* **36**, 268-272.

Singh, J. P. N. and Mittal, A. K. (1989). Structure and histochemistry of the dermis of a chequered water snake, *Natrix piscator*. *J. Zool. Lond.* **219**, 21-28.

Swartz, S. M., Groves, M. S., Kim, H. D. and Walsh, W. R. (1996). Mechanical properties of bat wing membrane skin. *J. Zool. Lond.* **239**, 357-378.

Wainwright, S. A., Vosburgh, F. and Hebrank, J. H. (1978). Shark skin: function in locomotion. *Science* **202**, 747-749.

Zanger, K., Schwinger, G. and Greven, H. (1995). Mechanical properties of the skin of *Rana esculenta* (Anura, Amphibia) with some notes on structures related to them. *Ann. Anat.* **177**, 509-514.